Supplementary material for the manuscript:

Incoherent dispersive shocks in the spectral evolution of random waves

Josselin Garnier[1,2], Gang Xu[3], Stefano Trillo[4], and Antonio Picozzi[3]

[1]*Ecole Normale Supérieure, Mathematics Department, CNRS, 45 rue d'Ulm, Paris, France*

[2]*Laboratoire de Probabilités et Modèles Aléatoires,*

University Paris Diderot, 75205 Paris Cedex 13, France

[3]*Laboratoire Interdisciplinaire Carnot de Bourgogne - CNRS,*

University of Burgundy, 21078 Dijon, France

[4]*Department of Engineering, University of Ferrara, Via Saragat 1, 44122 Ferrara, Italy*

In the first part of the Supplemental we report the general theory underlying the derivation of the singular integro-differential kinetic equations (SIDKE). In the second part we present complementary numerical simulations and discuss the feasibility of the optical experiment aimed at observing incoherent DSWs.

I. DERIVATION OF THE SINGULAR INTEGRO-DIFFERENTIAL KINETIC EQUATIONS

In this Section we describe in detail the mathematical procedure which allowed us to derive the singular integro-differential kinetic equations (SIDKE) starting from the kinetic equation (KE) given in Eq.(2) of the Letter. We first present the theory in the framework of a general response function (satisfying the causality property) and show that the leading-order terms of the SIDKE are related to the properties of the response function close to zero. Then we apply the general results to the damped harmonic oscillator response and the purely exponential response.

A. A general response function

The starting point is to carefully address the singularities involved in the convolution operator of the KE (2) in the Letter. The response function can be written in the following general form

$$R(t) = \frac{1}{\tau_R}\bar{R}\Big(\frac{t}{\tau_R}\Big)H(t),$$

where $H(t)$ denotes the Heaviside function and $\bar{R}$ is a smooth function (that is at least five times differentiable with integrable derivatives).

By using integration by parts one finds that the imaginary part of the Fourier transform of the response function

$$g_\omega = \mathrm{Im}\Big(\int_{-\infty}^{\infty} R(t)e^{-i\omega t}dt\Big)$$

has the form

$$g_\omega = g^0_{\omega\tau_R}, \qquad g^0_\omega = -\frac{1}{\omega}\bar{R}(0) + \frac{1}{\omega^3}\bar{R}^{(2)}(0) - \frac{1}{\omega^5}\bar{R}^{(4)}(0) - \frac{1}{\omega^5}\mathrm{Re}\Big(\int_0^{\infty}\bar{R}^{(5)}(t)e^{-i\omega t}dt\Big),$$

where $\bar{R}^{(j)}(t)$ denotes the $j-$th derivative of $\bar{R}(t)$. This allows us to identify the two 'singularities' (the terms in $1/\omega$ and $1/\omega^3$) that are important when addressing the convolution operator of the KE (2) in the Letter.

For a smooth function n_ω we want to find the expression of

$$N_\omega = \int_{-\infty}^{\infty} g_{\omega-u}n_u du, \tag{1}$$

in particular in the regime $\tau_R \gg 1$.

Summary of the general results:

1. For any $\tau_R > 0$, the convolution operator can be written in the following form without approximations

$$N_\omega = -\frac{\pi\bar{R}(0)}{\tau_R}\mathcal{H}n_\omega + \frac{\pi\bar{R}^{(1)}(0)}{\tau_R^2}\partial_\omega n_\omega + \frac{\pi\bar{R}^{(2)}(0)}{2\tau_R^3}\mathcal{H}\partial_\omega^2 n_\omega + \frac{1}{\tau_R^4}\int_0^\infty \big[\partial_\omega^3 n_{\omega+\frac{u}{\tau_R}} + \partial_\omega^3 n_{\omega-\frac{u}{\tau_R}}\big]G^0(u)du, \quad (2)$$

where we have defined for $u > 0$:

$$G^0(u) = -\frac{1}{2}\int_u^\infty \big(g_v^0 + \frac{\bar{R}(0)}{v} - \frac{\bar{R}^{(2)}(0)}{v^3}\big)(v-u)^2 dv, \quad (3)$$

and $\mathcal{H}$ is the Hilbert transform.

2. When $\tau_R \gg 1$,

$$N_\omega = -\frac{\pi\bar{R}(0)}{\tau_R}\mathcal{H}n_\omega + \frac{\pi\bar{R}^{(1)}(0)}{\tau_R^2}\partial_\omega n_\omega + \frac{\pi\bar{R}^{(2)}(0)}{2\tau_R^3}\mathcal{H}\partial_\omega^2 n_\omega - \frac{\pi\bar{R}^{(3)}(0)}{6\tau_R^4}\partial_\omega^3 n_\omega + o\Big(\frac{1}{\tau_R^4}\Big). \quad (4)$$

These results show that the leading-order term in the expansion (4) is determined by the behavior of the response function at 0. We will address in the two following sections two examples for which $\bar{R}(0) = 0$ and $\bar{R}(0) \neq 0$ [1], respectively.

Proof.

We can write N_ω in the form

$$\begin{aligned} N_\omega &= -\frac{\bar{R}(0)}{\tau_R}\mathcal{P}\int_{-\infty}^\infty n_{\omega-u}\frac{1}{u}du + \frac{1}{\tau_R}\mathcal{P}\int_{-\infty}^\infty \big(g_u^0 + \frac{\bar{R}(0)}{u}\big)n_{\omega-\frac{u}{\tau_R}}du \\ &= -\frac{\pi\bar{R}(0)}{\tau_R}\mathcal{H}n_\omega - \frac{1}{\tau_R}\int_0^\infty \big(g_u^0 + \frac{\bar{R}(0)}{u}\big)\big[n_{\omega+\frac{u}{\tau_R}} - n_{\omega-\frac{u}{\tau_R}}\big]du \\ &= -\frac{\pi\bar{R}(0)}{\tau_R}\mathcal{H}n_\omega - \frac{1}{\tau_R}\int_0^\infty \partial_u f^0(u)\big[n_{\omega+\frac{u}{\tau_R}} - n_{\omega-\frac{u}{\tau_R}}\big]du, \end{aligned}$$

where we have introduced the function f^0 defined by (for $u > 0$):

$$f^0(u) = -\int_u^\infty g_v^0 + \frac{\bar{R}(0)}{v}dv.$$

Note that f^0 can be expanded as $f^0(u) = -\frac{\bar{R}^{(2)}(0)}{2u^2} + O(\frac{1}{u^4})$ as $u \to \infty$ and $f^0(u) = \bar{R}(0)\ln u + O(1)$ as $u \to 0$, so that $\lim_{u\to 0} f^0(u)\big[n_{\omega+\frac{u}{\tau_R}} - n_{\omega-\frac{u}{\tau_R}}\big] = 0$. Therefore we can write after integration by parts

$$\begin{aligned} N_\omega &= -\frac{\pi\bar{R}(0)}{\tau_R}\mathcal{H}n_\omega + \frac{1}{\tau_R^2}\int_0^\infty f^0(u)\big[\partial_\omega n_{\omega+\frac{u}{\tau_R}} + \partial_\omega n_{\omega-\frac{u}{\tau_R}}\big]du \\ &= -\frac{\pi\bar{R}(0)}{\tau_R}\mathcal{H}n_\omega + \frac{\bar{f}}{\tau_R^2}\partial_\omega n_\omega + \frac{1}{\tau_R^2}\int_0^\infty f^0(u)\big[\partial_\omega n_{\omega+\frac{u}{\tau_R}} + \partial_\omega n_{\omega-\frac{u}{\tau_R}} - 2\partial_\omega n_\omega\big]du, \end{aligned}$$

where

$$\bar{f} = 2\int_0^\infty f^0(u)du = -\int_{-\infty}^\infty u g_u^0 + \bar{R}(0)du.$$

After integration by parts:

$$ug_u^0 + \bar{R}(0) = -\mathrm{Re}\Big(\int_0^\infty \bar{R}^{(1)}(t)e^{-iut}dt\Big),$$

and therefore

$$\bar{f} = \pi\bar{R}^{(1)}(0).$$

We can write

$$N_\omega \;=\; -\frac{\pi\bar{R}(0)}{\tau_R}\mathcal{H}n_\omega + \frac{\pi\bar{R}^{(1)}(0)}{\tau_R^2}\partial_\omega n_\omega + \frac{1}{\tau_R^2}\int_0^\infty \partial_u F^0(u)\big[\partial_\omega n_{\omega+\frac{u}{\tau_R}} + \partial_\omega n_{\omega-\frac{u}{\tau_R}} - 2\partial_\omega n_\omega\big]du,$$

where we have introduced the function F^0 defined by (for $u > 0$):

$$F^0(u) = -\int_u^\infty f^0(v)dv.$$

Note that F^0 can be expanded as $F^0(u) = \frac{\bar{R}^{(2)}(0)}{2u} + O(\frac{1}{u^3})$ as $u \to \infty$ and $F^0(u) = -\pi\bar{R}^{(1)}(0)/2 + o(1)$ as $u \to 0$, so that $\lim_{u\to 0} F^0(u)\big[\partial_\omega n_{\omega+\frac{u}{\tau_R}} + \partial_\omega n_{\omega-\frac{u}{\tau_R}} - 2\partial_\omega n_\omega\big] = 0$. Therefore, after integration by parts we find

$$\begin{aligned}
N_\omega \;&=\; -\frac{\pi\bar{R}(0)}{\tau_R}\mathcal{H}n_\omega + \frac{\pi\bar{R}^{(1)}(0)}{\tau_R^2}\partial_\omega n_\omega - \frac{1}{\tau_R^3}\int_0^\infty F^0(u)\big[\partial_\omega^2 n_{\omega+\frac{u}{\tau_R}} - \partial_\omega^2 n_{\omega-\frac{u}{\tau_R}}\big]du \\
&=\; -\frac{\pi\bar{R}(0)}{\tau_R}\mathcal{H}n_\omega + \frac{\pi\bar{R}^{(1)}(0)}{\tau_R^2}\partial_\omega n_\omega + \frac{\pi\bar{R}^{(2)}(0)}{2\tau_R^3}\mathcal{H}\partial_\omega^2 n_\omega \\
&\quad -\frac{1}{\tau_R^3}\int_0^\infty \big(F^0(u) - \frac{\bar{R}^{(2)}(0)}{2u}\big)\big[\partial_\omega^2 n_{\omega+\frac{u}{\tau_R}} - \partial_\omega^2 n_{\omega-\frac{u}{\tau_R}}\big]du \\
&=\; -\frac{\pi\bar{R}(0)}{\tau_R}\mathcal{H}n_\omega + \frac{\pi\bar{R}^{(1)}(0)}{\tau_R^2}\partial_\omega n_\omega + \frac{\pi\bar{R}^{(2)}(0)}{2\tau_R^3}\mathcal{H}\partial_\omega^2 n_\omega - \frac{1}{\tau_R^3}\int_0^\infty \partial_u G^0(u)\big[\partial_\omega^2 n_{\omega+\frac{u}{\tau_R}} - \partial_\omega^2 n_{\omega-\frac{u}{\tau_R}}\big]du,
\end{aligned}$$

where we have introduced

$$G^0(u) = -\int_u^\infty F^0(v) - \frac{\bar{R}^{(2)}(0)}{2v}dv.$$

After some calculations, this expression of $G^0(u)$ can be written in the form given in Eq.(3). Note that $G^0(u) = O(\frac{1}{u^2})$ as $u \to \infty$ and $G^0(u) = O(\ln u)$ as $u \to 0$, so that $\lim_{u\to 0} G^0(u)\big[\partial_\omega^2 n_{\omega+\frac{u}{\tau_R}} - \partial_\omega^2 n_{\omega-\frac{u}{\tau_R}}\big] = 0$ and we can integrate by parts the last term

$$N_\omega \;=\; -\frac{\pi\bar{R}(0)}{\tau_R}\mathcal{H}n_\omega + \frac{\pi\bar{R}^{(1)}(0)}{\tau_R^2}\partial_\omega n_\omega + \frac{\pi\bar{R}^{(2)}(0)}{2\tau_R^3}\mathcal{H}\partial_\omega^2 n_\omega + \frac{1}{\tau_R^4}\int_0^\infty G^0(u)\big[\partial_\omega^3 n_{\omega+\frac{u}{\tau_R}} + \partial_\omega^3 n_{\omega-\frac{u}{\tau_R}}\big]du,$$

which is the first desired result. This expression of N_ω is exact, and G^0 is an integrable function over $(0,\infty)$. As a result N_ω has the following expansion as $\tau_R \gg 1$:

$$N_\omega \;=\; -\frac{\pi\bar{R}(0)}{\tau_R}\mathcal{H}n_\omega + \frac{\pi\bar{R}^{(1)}(0)}{\tau_R^2}\partial_\omega n_\omega + \frac{\pi\bar{R}^{(2)}(0)}{2\tau_R^3}\mathcal{H}\partial_\omega^2 n_\omega + \frac{\bar{G}}{\tau_R^4}\partial_\omega^3 n_\omega + o\Big(\frac{1}{\tau_R^4}\Big),$$

with

$$\bar{G} = 2\int_0^\infty G^0(u)du = -\frac{1}{6}\int_{-\infty}^{\infty} u^3 g_u^0 + u^2\bar{R}(0) - \bar{R}^{(2)}(0)du.$$

After iterated integration by parts:

$$u^3 g_u^0 + u^2\bar{R}(0) - \bar{R}^{(2)}(0) = \mathrm{Re}\Big(\int \bar{R}^{(3)}(t)e^{-iut}dt\Big),$$

and therefore

$$\bar{G} = -\frac{\pi}{6}\bar{R}^{(3)}(0),$$

which completes the proof.

B. Damped harmonic oscillator response

In this Section we apply the general theory exposed here above to the particular example of a damped harmonic oscillator response function. In this way we derive the SIDKEs reported in Eqs.(3,4) of the Letter. The normalized nonlinear response function is $R(t) = \frac{1+\beta^2}{\beta\tau_R}\sin(\beta t/\tau_R)\exp(-t/\tau_R)H(t)$, where we recall that $H(t)$ denotes the Heaviside function. The imaginary part of its Fourier transform $g_\omega = \mathrm{Im}\Big(\int_{-\infty}^{\infty} R(t)e^{-i\omega t}dt\Big)$ is

$$g_\omega = \frac{1+\beta^2}{2\beta}\Big(\frac{1}{1+(\beta+\tau_R\omega)^2} - \frac{1}{1+(\beta-\tau_R\omega)^2}\Big). \tag{5}$$

For a smooth function n_ω we want to find the expression of

$$N_\omega = \int_{-\infty}^{\infty} g_{\omega-u}n_u du, \tag{6}$$

in particular in the regime $\tau_R \gg 1$. Applying the general theory reported in the previous section, we find the following results.

1. For any $\tau_R, \beta > 0$,

$$N_\omega = \frac{\pi(1+\beta^2)}{\tau_R^2}\partial_\omega n_\omega - \frac{\pi(1+\beta^2)}{\tau_R^3}\mathcal{H}\partial_\omega^2 n_\omega + \frac{1}{\tau_R^4}\int_0^\infty \big[\partial_\omega^3 n_{\omega+\frac{u}{\tau_R}} + \partial_\omega^3 n_{\omega-\frac{u}{\tau_R}}\big]G^0(u)du, \tag{7}$$

where we have defined for $u > 0$:

$$G^0(u) = \frac{1+\beta^2}{\beta}\int_u^\infty \frac{\pi\beta}{2} - \frac{1}{2}\Big[w\arctan(w) - \frac{1}{2}\log(1+w^2)\Big]_{v-\beta}^{v+\beta} - \frac{\beta}{v}dv, \tag{8}$$

and $\mathcal{H}$ is the Hilbert transform.

2. When $\tau_R \gg 1$,

$$N_\omega = \frac{\pi(1+\beta^2)}{\tau_R^2}\partial_\omega n_\omega - \frac{\pi(1+\beta^2)}{\tau_R^3}\mathcal{H}\partial_\omega^2 n_\omega - \frac{1+\beta^2}{2\tau_R^4}\partial_\omega^3 n_\omega + o\Big(\frac{1}{\tau_R^4}\Big). \tag{9}$$

- SIDKE without background: Eq.(3) in the Letter

With an initial condition without background:

$$n_\omega(z=0) \overset{\omega\to\pm\infty}{\longrightarrow} 0, \tag{10}$$

in the asymptotic regime $\tau_R \gg 1$, the spectrum satisfies the SIDKE

$$\partial_z n_\omega = \frac{1+\beta^2}{\tau_R^2}\left(n_\omega \partial_\omega n_\omega - \frac{1}{\tau_R} n_\omega \mathcal{H}\partial_\omega^2 n_\omega - \frac{1}{2\pi\tau_R^2} n_\omega \partial_\omega^3 n_\omega\right), \tag{11}$$

in which the second term is dispersive and thus regularizes the (first) shock term in the rhs of Eq.(11).

Although the third term is perturbative with respect to the second term, its third-order derivatives can play a non-negligible role in the long-term dynamics, when the width of the spectral peaks that emerge from the DSW become of the order of the width of the gain spectrum, $\Delta\omega_g$. We qualitatively assess the roles of the three terms through the analysis of the three corresponding propagation lengths $(L_j, j = 1, 2, 3)$ over which they play a non-negligible role. We have $L_1 \sim \tau_R^2 \Delta\omega/\bar{n}$, $L_2 \sim \tau_R^3 \Delta\omega^2/\bar{n}$, and $L_3 = \tau_R^4 \Delta\omega^3/\bar{n}$, where $\Delta\omega$ denotes the typical frequency scale of variations of n_ω and $\bar{n}$ its typical amplitude. The derivation of the SIDKE (11) is based on a multi-scale expansion, which remains well-ordered if $L_1/L_2 \ll 1$ and $L_2/L_3 \ll 1$, i.e., $\Delta\omega \gg 1/\tau_R \sim \Delta\omega_g$. Then the third term of the SIDKE (11) remains negligible during the whole development of the incoherent shock, while it becomes of the same order as the other two terms in the long-term dynamics, when the widths of the spectral peaks emerging from the shock become comparable to $\Delta\omega_g$ (see Fig. 1d in the Letter).

- SIDKE with background: Eq.(4) in the Letter

With an initial condition with background:

$$n_\omega(z) = n_0 + \tilde{n}_\omega(z), \qquad n_0 > 0, \tag{12}$$

introducing the scaling

$$\tilde{n}_\omega(z) = \frac{1}{\tau_R}\tilde{n}_\omega^{(0)}(z/\tau_R^3), \tag{13}$$

the spectrum satisfies in the asymptotic regime $\tau_R \gg 1$

$$\partial_Z \tilde{n}_\omega^{(0)} = (1+\beta^2)\big(\tau_R n_0 \partial_\omega \tilde{n}_\omega^{(0)} + \tilde{n}_\omega^{(0)} \partial_\omega \tilde{n}_\omega^{(0)} - n_0 \mathcal{H}\partial_\omega^2 \tilde{n}_\omega^{(0)}\big). \tag{14}$$

where $Z = z/\tau_R^3$. The first term of this equation can be removed by a change of Galilean reference frame, $(\Omega = \omega + (1+\beta^2)\tau_R n_0 Z, \xi = Z)$, so that Eq.(14) recovers the Benjamin-Ono (BO) equation.

To compare the simulations of Eq.(14) with those of the KE (2), we come back to the original variables, which gives

$$\tau_R^2\partial_z\tilde{n}_\omega - (1+\beta^2)n_0\partial_\omega\tilde{n}_\omega = (1+\beta^2)\big(\tilde{n}_\omega\partial_\omega\tilde{n}_\omega - \frac{1}{\tau_R}n_0\mathcal{H}\partial_\omega^2\tilde{n}_\omega\big). \tag{15}$$

This BO-like equation is completely integrable [3], and thus admits soliton solutions and an infinite number of conserved quantities. *Note that the BO equation finds a timely application to model submerged plumes of oil as were reported following the Deepwater Horizon leak in the Gulf of Mexico in May 2010.* This problem is discussed in particular by P.D. Miller in relation with recent on line video experiments [4].

C. Exponential response

In this Section we apply the general theory reported above in Section I to the particular example of a purely exponential response function. In this way we derive the SIDKEs reported in Eqs.(5,6) of the Letter. Note that an exponential response function is found whenever one models the medium by means of a simple rate equation, see e.g., Maxwell-Debye model, Maxwell-Bloch equations, or the two temperature model in the context of condensed matter physics [2].

The nonlinear response function is $R(t) = H(t)\frac{1}{\tau_R}\exp\big(-\frac{t}{\tau_R}\big)$, and the imaginary part of its Fourier transform $g_\omega = \mathrm{Im}\Big(\int_{-\infty}^{\infty}R(t)e^{-i\omega t}dt\Big)$ reads

$$g_\omega = -\frac{\tau_R\omega}{1+(\tau_R\omega)^2}. \tag{16}$$

For a smooth function n_ω we want to find the expression of

$$N_\omega = \int_{-\infty}^{\infty} g_{\omega-u}n_u du, \tag{17}$$

in particular in the regime $\tau_R \gg 1$. Applying the general results derived in the previous section, we find the following results.

1. For any $\tau_R > 0$,

$$N_\omega = -\frac{\pi}{\tau_R}\mathcal{H}n_\omega - \frac{\pi}{\tau_R^2}\partial_\omega n_\omega + \frac{\pi}{2\tau_R^3}\mathcal{H}\partial_\omega^2 n_\omega + \frac{1}{\tau_R^4}\int_0^\infty \big[\partial_\omega^3 n_{\omega+\frac{u}{\tau_R}} + \partial_\omega^3 n_{\omega-\frac{u}{\tau_R}}\big]G^0(u)du, \tag{18}$$

where we have defined for $u > 0$:

$$G^0(u) \;=\; -\frac{3}{4} + \frac{1}{4}(1-u^2)\ln\Big(1+\frac{1}{u^2}\Big) + u\arctan\Big(\frac{1}{u}\Big). \tag{19}$$

2. When $\tau_R \gg 1$,

$$N_\omega = -\frac{\pi}{\tau_R}\mathcal{H}n_\omega - \frac{\pi}{\tau_R^2}\partial_\omega n_\omega + \frac{\pi}{2\tau_R^3}\mathcal{H}\partial_\omega^2 n_\omega + \frac{\pi}{6\tau_R^4}\partial_\omega^3 n_\omega + o\Big(\frac{1}{\tau_R^4}\Big). \tag{20}$$

1. From the convolution operator to SIDKEs

The starting point is again the KE (2) in the Letter.

$$\partial_z n_\omega = \frac{1}{\pi} n_\omega \int g_{\omega-u} n_u du. \tag{21}$$

- SIDKE without background: Eq.(5) in the Letter

With an initial condition without background:

$$n_\omega(z=0) = \tilde{n}^0_\omega, \qquad \text{with } \tilde{n}^0_\omega \overset{\omega\to\pm\infty}{\longrightarrow} 0, \tag{22}$$

in the asymptotic regime $\tau_R \gg 1$, the spectrum satisfies the SIDKE (5) in the Letter

$$\tau_R \partial_z n_\omega = -n_\omega \mathcal{H} n_\omega - \frac{1}{\tau_R} n_\omega \partial_\omega n_\omega + \frac{1}{2\tau_R^2} n_\omega \mathcal{H} \partial^2_\omega n_\omega. \tag{23}$$

As discussed in the Letter, the dynamics is dominated by the leading-order term in the rhs of Eq.(23):

$$\partial_{\tilde{z}} n_\omega = -n_\omega \mathcal{H} n_\omega \tag{24}$$

with $\tilde{z} = z/\tau_R$. The numerical simulations of this equation show that the spectrum exhibits a collapse-like dynamics which is saturated in the presence of a small amplitude background. There is local existence and uniqueness of the solution, but global existence is not guaranteed when there is no background. Actually, Constantin, Lax and Majda constructed a one-dimensional model of the vorticity formulation of the 3D Euler equations that has the form of Eq.(24) [5]. For a given initial condition $n_\omega(z=0) = n^0_\omega$ the solution has the form

$$n_\omega(\tilde{z}) = \frac{4 n^0_\omega}{(2 + \tilde{z}\mathcal{H} n^0_\omega)^2 + \tilde{z}^2 (n^0_\omega)^2}. \tag{25}$$

There is blow up if and only if there exists ω such that $n^0_\omega = 0$ and $\mathcal{H} n^0_\omega < 0$. Then the blow up distance $\tilde{z}_c$ is given by $\tilde{z}_c = -2/[\mathcal{H} n^0_{\omega=\omega_0}]$, where ω_0 is such that $n^0_{\omega_0} = 0$. If the initial condition n^0_ω vanishes for several frequencies, then $2/\tilde{z}_c = \sup\{-\mathcal{H} n^0_\omega\,,\ \omega \text{ s.t. } n^0_\omega = 0\}$.

If the initial condition is Lorentzian:

$$n^0_\omega = \frac{N\omega_0}{\pi(\omega_0^2 + \omega^2)}$$

with $N = \int n^0_\omega d\omega$, then the solution propagates with constant shape and constant velocity

$$n_\omega(\tilde{z}) = \frac{N\omega_0}{\pi(\omega_0^2 + (\omega - \tilde{c}_0 \tilde{z})^2)}$$

with $\tilde{c}_0 = -N/(2\pi)$. If the initial condition is positive-valued and has the form of a peak that decays to zero at infinity faster than a Lorentzian, then there is no blow up, but the solution exhibits a peak that

moves towards the left tail of the initial spectrum n_ω^0 at velocity $\tilde{c}_0$ (see the Letter). More generally, if the initial condition n_ω^0 decays fast enough, then denoting

$$\langle \omega^p \rangle = \frac{1}{N}\int \omega^p n_\omega(z) d\omega, \qquad \langle \omega_0^p \rangle = \frac{1}{N}\int \omega^p n_\omega^0 d\omega$$

and assuming $\langle \omega_0^p \rangle = 0$ for odd p, we have

$$\begin{aligned}
\langle \omega \rangle &= \tilde{c}_0 \tilde{z}, \\
\left\langle (\omega - \langle \omega \rangle)^2 \right\rangle &= \left\langle \omega_0^2 \right\rangle, \\
\left\langle (\omega - \langle \omega \rangle)^3 \right\rangle &= -\left\langle \omega_0^2 \right\rangle \tilde{c}_0 \tilde{z}, \\
\left\langle (\omega - \langle \omega \rangle)^4 \right\rangle &= \left\langle \omega_0^4 \right\rangle + \left\langle \omega_0^2 \right\rangle \tilde{c}_0^2 \tilde{z}^2,
\end{aligned}$$

which shows that the spectrum moves with velocity $\tilde{c}_0$ but also experiences an asymmetric deformation.

It is interesting to note that, in contrast with conventional coherent DSWs, which usually require a background, here, it is the absence of the (noise) background which leads to a singularity. On the other hand, we will now see that this singularity is suppressed by the existence of a non-vanishing background.

- SIDKE with background: Eq.(6) in the Letter

With an initial condition with background:

$$n_\omega(z) = n_0 + \tilde{n}_\omega(z), \qquad n_0 > 0, \tag{26}$$

introducing the scaling

$$\tilde{n}_\omega(z) = \frac{1}{\tau_R}\tilde{n}_\omega^{(0)}(z/\tau_R), \tag{27}$$

the spectrum satisfies in the asymptotic regime $\tau_R \gg 1$

$$\partial_Z \tilde{n}_\omega^{(0)} = -n_0 \mathcal{H}\tilde{n}_\omega^{(0)} - \frac{1}{\tau_R}\Big(\tilde{n}_\omega^{(0)}\mathcal{H}\tilde{n}_\omega^{(0)} + n_0 \partial_\omega \tilde{n}_\omega^{(0)}\Big) + \frac{1}{\tau_R^2}\Big(- \tilde{n}_\omega^{(0)}\partial_\omega \tilde{n}_\omega^{(0)} + \frac{1}{2} n_0 \mathcal{H}\partial_\omega^2 \tilde{n}_\omega^{(0)}\Big). \tag{28}$$

where $Z = z/\tau_R$. The leading-order linear term is

$$\partial_Z \tilde{n}_\omega^{(0)} = -n_0 \mathcal{H}\tilde{n}_\omega^{(0)}. \tag{29}$$

The solution to this linear equation is periodic

$$\tilde{n}_\omega^{(0)}(Z) = \cos\big(n_0 Z\big)\tilde{n}_{\omega,0}^{(0)} - \sin\big(n_0 Z\big)\mathcal{H}\tilde{n}_{\omega,0}^{(0)}, \tag{30}$$

where $\tilde{n}_\omega^{(0)}(Z=0) = \tilde{n}_{\omega,0}^{(0)}$. It turns out that the presence of a background, $n_0 \gg \tilde{n}_\omega$, removes the collapse singularity discussed above through Eq.(25).

In order to compare this solution with the simulations of the whole SIDKE (28), of the KE (2) and of the NLS Eq.(1), we need to come back to the original variables, which gives the SIDKE (6) and the analytical periodic solution (7) in the Letter.

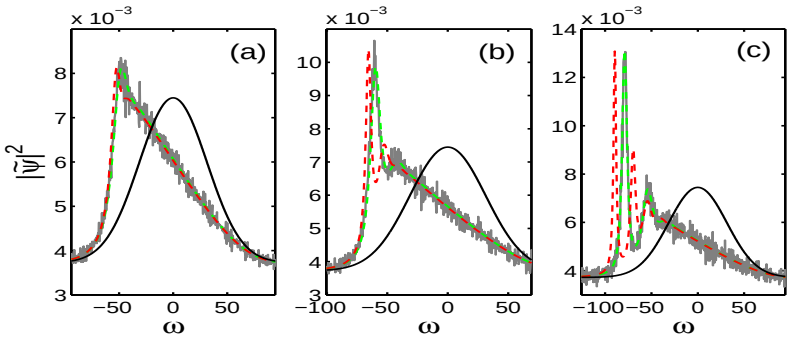

FIG. 1: Simulations of the NLSE (grey), KE (green) and BO (dashed red) equations for $\tau_R = 1$ ($\beta = 1, \sigma = 1$, the damped harmonic oscillator response is considered here). A quantitative agreement is obtained between the NLSE and the KE. Because of the small value of τ_R, a discrepancy is observed with the BO equation. The spectra refer to $z = 7000$ (a), $z = 10000$ (b), $z = 15000$ (c), $z = 20000$ (d). The dark line refers to the initial condition.

II. COMPLEMENTARY NUMERICAL SIMULATIONS

In this Section we complete the numerical study reported in the Letter. We report numerical simulations of the NLSE, of the KE and of the SIDKE in different conditions. First of all, *we would like to underline again that all comparisons between these equations have been reported without making use of any adjustable parameter*. Note that, in order to compare the NLSE simulations with those of the KE and SIDKEs, a simple averaging over nearest-neighbour points has been used in the plots of the stochastic NLSE spectra. We have verified that other smoothing algorithms, such as the Savitzky-Golay smoothing filter, the moving average, or the Loess algorithm, provide almost identical results.

A. Role of the response time τ_R

In the Letter, we have considered moderate values of the parameter τ_R ($\tau_R = 3$ or $\tau_R = 5$), and a good agreement has been obtained between the NLSE, KE and SIDKEs. Here we show that for smaller values of the parameter $\tau_R (\sim 1)$, a quantitative agreement is still obtained between the NLSE and the KE, while the spectral evolutions obtained with these equations deviates from the predictions of the SIDKEs. *This is obviously consistent with the multi-scale expansion which underlies the derivation of SIDKEs*. We illustrate this in Fig. 1 by considering the example of the damped harmonic oscillator with background (where the SIDKE refers to the BO equation), while similar results have been obtained without

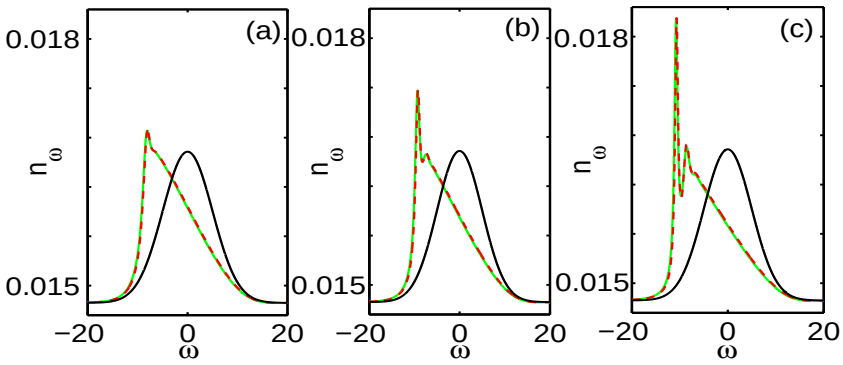

FIG. 2: Simulations of the KE (green) and BO (red) equations for $\tau_R = 10$ ($\beta = 1, \sigma = 1$, the damped harmonic oscillator response is considered here). A quantitative agreement is obtained between the KE and the BO equation. The spectra refer to $z = 1.61 \times 10^6$ (a), $z = 2 \times 10^6$ (b), $z = 2.5 \times 10^6$ (c). The dark line refers to the initial condition.

background. Conversely, for large values of the parameter τ_R, the rapid spectral oscillations produced by the DSW become very narrow and thus invalidate the weakly nonlinear approximation which underlies the derivation of the KE. A discrepancy is observed in this case between the simulations of the NLSE and the KE. On the other hand, as remarkably illustrated in Fig. 2, an excellent quantitative agreement is obtained between the simulations of the KE and the BO equation, as expected from the multi-scale expansion with the small parameter $1/\tau_R$.

Let us finally comment the long term evolution of the DSW discussed in Fig. 3 of the Letter. In this case the DSW asymptotically leads to the the generation of genuine BO solitons, as confirmed by the simulation reported here in Fig. 3. Accordingly, the amplitudes of the peaks that emerge from the DSW saturate to a constant value in their long-term evolution (Fig. 3d), a feature which is in contrast with the non-solitonic DSW discussed through Fig. 1 in the Letter. It is interesting to note in Fig. 3 that, during the shock, a quantitative agreement is obtained between the simulations of the BO equation and those of the KE (see Fig. 3a-b), whereas an appreciable discrepancy arises once solitons are generated in the long term (post-shock) dynamics (see Fig. 3c). This is simply due to the limited range of validity of the reduced BO equation: as the solitons form, their widths become comparable to the width of the gain spectrum ($\Delta\omega \sim \Delta\omega_g$), while their amplitudes become comparable to the background noise level ($\tilde{n}_\omega \sim n_0$). Although the validity of the approximations underlying the derivation of the BO equation becomes critiquable, we note in Fig. 3 that the BO equation still provides a reliable qualitative description of the long term evolution of the DSW.

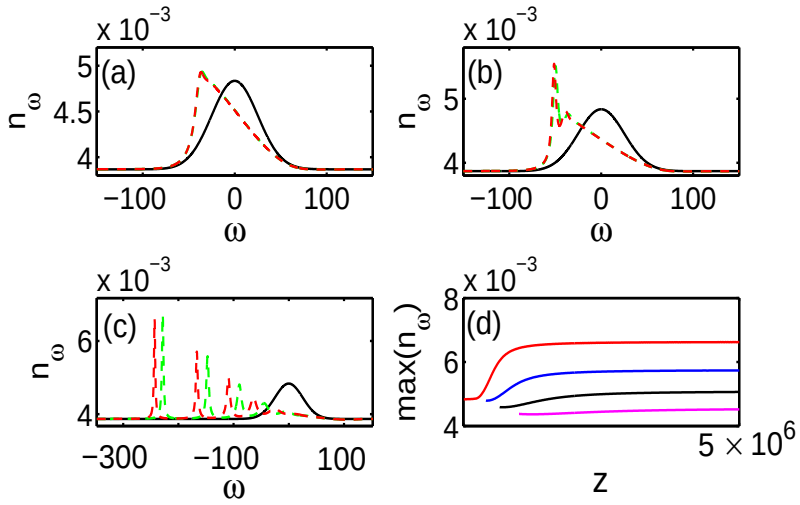

FIG. 3: (a-c) Long-term evolution of the solitonic DSW: Simulation of the KE (green) and BO (red) with a bright initial condition ($\tau_R = 4, \beta = 1, \sigma = 1$, damped harmonic oscillator response). The DSW eventually leads to the generation of BO soliton states, as attested by the evolutions of the maximum amplitudes of the first few peaks (d). See the text for a discussion of the discrepancy between the BO and KE simulations. (a) $z = 3 \times 10^5$, (b) $z = 5 \times 10^5$, (c) $z = 2.8 \times 10^6$.

B. Relation with spectral incoherent solitons

The so-called 'spectral incoherent solitons' have been studied theoretically and experimentally in different circumstances in the context of optics [6–8]. A necessary condition for the generation of a spectral incoherent soliton is the existence of a noise background, say n_∞, which prevents the process of spectral narrowing and amplification of the peaks discussed through Fig. 1d in the Letter. This is illustrated in the numerical simulations of the KE (2) reported here below in Fig. 4. It has been realized in the same conditions as Fig. 1d in the Letter, except that the initial Gaussian spectrum has been superposed on a small-amplitude noise background. It shows that the amplification of the spectral peaks is arrested once they reach the small-amplitude background, thus leading to the formation of spectral incoherent solitons (see Fig. 4b). This conclusion is corroborated by the analytical solitary-wave solution of the KE (2) discussed in Ref.[7]

$$n_\omega(z) - n_\infty = \big(n_m - n_\infty\big) \exp\Big[- \log\Big(\frac{n_m}{n_\infty}\Big) \frac{(\omega - Vz)^2}{\omega_{\rm i}^2}\Big],$$

where $n_m (\gg n_\infty)$ is the soliton peak amplitude, and the velocity of the solitary wave is

$$V = -\frac{n_m - n_\infty}{\log^{3/2}\left(\frac{n_m}{n_\infty}\right)} \frac{\gamma g_{\rm i} \omega_{\rm i}^2}{\sqrt{\pi}},$$

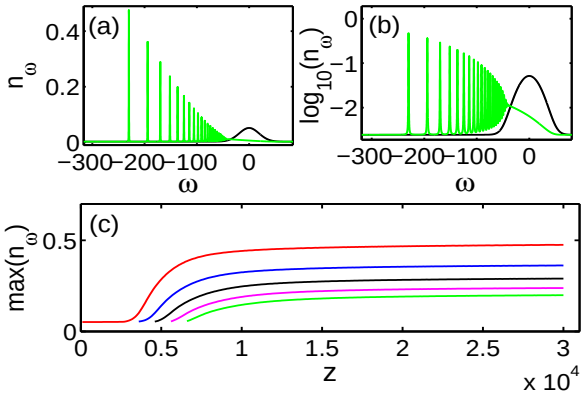

FIG. 4: Numerical simulations of the KE [Eq.(2) in the Letter] showing the evolution of the spectrum n_ω in normal (a), and logarithmic scale (b) ($z = 30\,000$), and corresponding evolutions of the maxima of the first few peaks (c). The simulation has been realized in the same conditions as Fig. 1 in the Letter, except that the initial Gaussian spectrum evolves in the presence of a small-amplitude noise background [see panel (b)]. The increase of the amplitudes of the spectral peaks slowly saturate once they reach the small-amplitude background, thus leading to the formation of a wave-train of spectral incoherent solitons.

where g_i and ω_i are constant parameters defined from the response function $R(t)$ [7]. This solution then explicitly shows that a noise background n_∞ sustains a stationary solitary-wave structure.

C. Supplement on the periodic behavior (Fig. 4b-c in the Letter)

We complete here the simulations concerning the periodic spectral behavior reported in Fig. 4b-c of the Letter for an exponential response function with background. We report in Fig. 5 the simulation of the NLSE, and the KE, as well as the simulation of the whole SIDKE [Eq.(6) in the Letter] and the plot of the analytical solution of the first term of this SIDKE [Eq.(7) in the Letter]. It is interesting to note that the collapse-like dynamics described by the second-term of the SIDKE [Eq.(6) in the Letter] is quenched by the corresponding leading-order term, which describes a periodic evolution. We underline the excellent agreement obtained between the different equations.

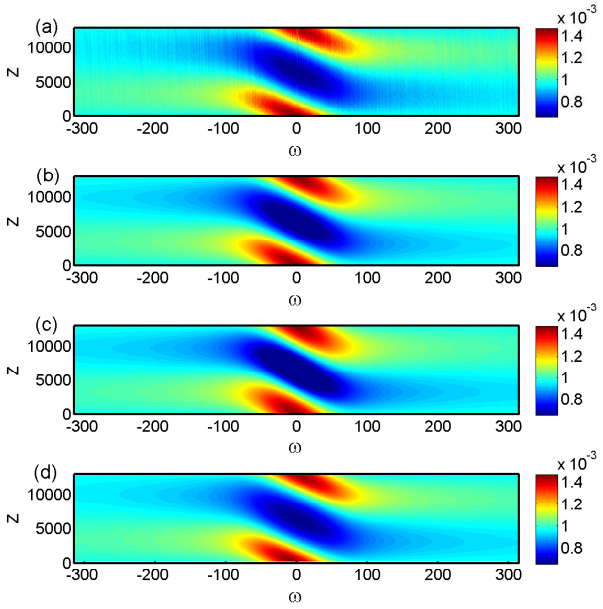

FIG. 5: Numerical simulations of the NLSE (a), KE (b), SIDKE [Eq.(6) in the Letter] (c), and plot of the analytical solution due to the leading-order term of the SIDKE (d) [Eq.(7) in the Letter]. An exponential response function with background is considered here ($\tau_R = 10$).

D. Complement on the experimental feasibility

Here we provide some more information concerning the feasibility of the experiment aimed at observing incoherent DSWs in the context of optical waves. It is important to underline that DSWs can be observed by exploiting the natural Raman effect in highly nonlinear fibers, such as photonic crystal fibers. To illustrate this, we report in Fig. 6 the numerical simulation of the generalized NLSE with the usual complete response function [9, 10], which includes an electronic (instantaneous) Kerr contribution as well as the molecular (retarded) Raman contribution

$$R(t) = (1 - f_R)\delta(t) + f_R H(t)\tau_1(\tau_1^{-2} + \tau_2^{-2})\exp(-t/\tau_2)\sin(t/\tau_1), \tag{31}$$

with $f_R = 0.18$, $\tau_1 = 12.2$fs, $\tau_2 = 32$fs [9, 10]. The complexity of this Raman response function (31) stems from the amorphous nature of silica glass. Note that, by showing the existence of Raman induced DSWs, our analysis reveals that these incoherent shocks are robust and can even be sustained by complicated response functions.

The numerical simulation corresponds to the following realistic experimental parameters. We considered a commercially available photonic crystal fiber with a nonlinear coefficient of $\gamma = 100\text{W}^{-1}\text{km}^{-1}$, and a

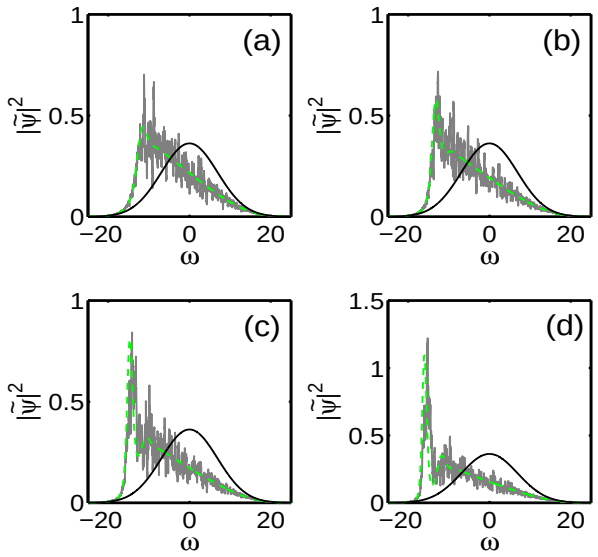

FIG. 6: Experimental feasibility: Numerical simulations of the generalized NLSE (gray) and the KE (dashed green) showing the formation of an incoherent DSW. The response function includes both an electronic instantaneous Kerr contribution and a delayed Raman contribution [see Eq.(31)]. (a) $z = 200L_{nl} = 2.42$m, (b) $z = 250L_{nl} = 3.05$m, (c) $z = 300L_{nl} = 3.66$m, (d) $z = 350L_{nl} = 4.27$m. We underline the quantitative agreement between the NLSE and the KE without adjustable parameters. This good agreement has been obtained in spite of the complexity of the response function (31).

second-order dispersion coefficient of $\beta_2 = 10^{-26}\text{s}^2/\text{m}$ (i.e., $\tau_0 = 11.1$fs, $L_{nl} = 1.22$cm, $\tau_R = 1.1\tau_0$). The source is an incoherent quasi-cw ($\sim$ ns pulse) of average power ~ 820W, and spectral bandwidth 97THz. In this way, the source exhibits a stationary statistics, in the sense that its time correlation is much shorter than the pulse duration. This kind of broadband incoherent sources are experimentally accessible by exploiting high-power quasi-cw supercontinuum generation in photonic crystal fibers, see, e.g., Refs.[9–12]. We remark in Fig. 6 that a fiber length as short as $L \simeq 5$m is sufficient to observe the formation of the incoherent dispersive shock wave.

We also reported in Fig. 6 the numerical simulation of the KE [Eq.(2) in the Letter]. A quantitative agreement has been obtained with the corresponding simulation of the generalized NLSE, without adjustable parameters and despite the complexity of the response function (31). Actually, the weakly nonlinear statistical approach shows that the instantaneous Kerr effect in (31) only contributes to the kinetic equation in a second-order perturbation theory in $\varepsilon = L_d/L_{nl}$. Accordingly, it does not contribute to the kinetic equation, which refers to a first-order closure of the hierarchy of moments equations (see Ref.[13] for more details).

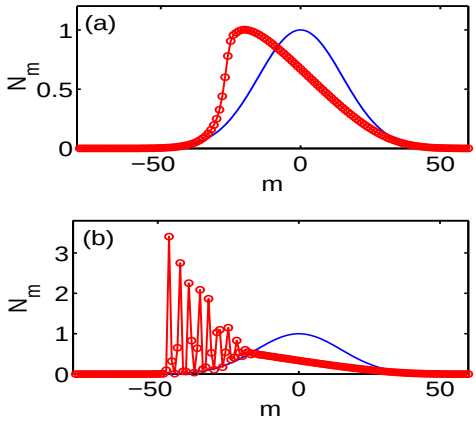

FIG. 7: Simulation of Eq.(32), which refers to a reduced model of the discrete Lotka-Volterra equation. The dynamics reveals the development of a shock structure, whose 'wave breaking' is subsequently regularized by the formation of rapid discrete oscillations [$g_0 = 1$, (a) $t = 10$, (b) $t = 33$, the initial condition is in blue].

Finally note that the experimental observation of incoherent DSWs can also be envisaged by exploiting the recent progress made on the fabrication of photonic crystal fibers filled with molecular liquids [14]. Indeed, molecular liquids usually display much larger nonlinear response times (τ_R is in the picosecond range) as compared to the Raman effect in silica fibers, so that the spectral bandwidth of the incoherent source can be reduced in a substantial way in this experimental configuration.

E. Complement on the discrete DSWs in the Lotka-Volterra model

We briefly comment here on the applicability of the ideas of DSWs to the discrete Lotka-Volterra model discussed in the conclusion of the Letter, $\partial_t n_j = n_j \sum_i g_{ji} n_i$ with $g_{ji} = -g_{ij}$. In order to map the limit $\tau_R \gg 1$, we need to consider the example of a nearest neighbor predator-prey interaction. In this case, the discrete Lotka-Volterra equation recovers the following simplified form

$$\dot{N}_m(t) = g_0 N_m \big(N_{m+1} - N_{m-1}\big), \tag{32}$$

where the dot denotes the derivative with respect to the time variable, t. This model was shown to be completely integrable by the inverse scattering method [15].

We have performed numerical simulations of Eq.(32). As illustrated in Fig. 7, the simulations indicate the existence of a discrete shock phenomenon: For a sufficiently broad initial condition, $N_m(t)$ exhibits a self-steepening process, whose 'wave-breaking' is subsequently regularized by the formation of rapid

discrete oscillations. The relation between these discrete structures and the corresponding discrete solitons solutions of the integrable model (32) will be the subject of future investigations.

---

[1] Note that the condition $\bar{R}(0) \neq 0$ arises whenever the 'excitation time' of a system is much smaller than the other relevant time scales, e.g., the time correlation of the incoherent wave. It is instructive to illustrate this aspect by considering the two temperature model (TTM), which is known to describe a non-equilibrium state between photo-excited electrons and lattice phonons in condensed matter. A simple version of the response function underlying the TTM reads, $R(t) = H(t)(e^{-t/\tau_e} - e^{-t/\tau_R})/(\tau_e - \tau_R)$ [2], where $\tau_e (< \tau_R)$ denotes the 'excitation time' (the time required to bring the system out of equilibrium), while τ_R denotes the relaxation time required to recover the equilibrium state. We have verified by numerical simulations of the NLSE and KE that when τ_e is much larger than the time correlation of the incoherent wave, $\tau_e \sim \tau_R \gg t_c$, then the field exhibits an incoherent DSW analogous to that discussed for the damped harmonic oscillator response (Fig. 1 in the Letter). Conversely, when $\tau_e \ll t_c$, the response function behaves as a pure exponential (though it is still continuous at $t = 0$), and the incoherent wave exhibits a collapse-like behavior completely analogous to that discussed for a discontinuous exponential response function (Fig. 4 in the Letter).

[2] A. Marini, M. Conforti, G. Della Valle, H. W. Lee, Tr. X. Tran, W. Chang, M. A. Schmidt, S. Longhi, P. St. J. Russell, and F. Biancalana, New J. Phys. **15**, 013033 (2013).

[3] A. Fokas, M. Ablowitz, Stud. Appl. Math. **68**, 1 (1983).

[4] P.D. Miller, Z. Xu, Comm. Math. Science **10**, 1 117 (2012). On line video experiments are reported by R. Camassa and R. McLaughlin, *How do underwater oil plumes form?*, http://www.youtube.com/watch?v=6Cp6fHINQ94

[5] P. Constantin, P. Lax and A. Majda, Comm. Pure Appl. Math. **38**, 715-724 (1985).

[6] A. Picozzi, S. Pitois, G. Millot, Phys. Rev. Lett. **101**, 093901 (2008).

[7] J. Garnier, A. Picozzi, Phys. Rev. A, **81**, 033831 (2010).

[8] B. Kibler, C. Michel, A. Kudlinski, B. Barviau, G. Millot, A. Picozzi, Phys. Rev. E **84**, 066605 (2011).

[9] G.P. Agrawal, *Nonlinear Fiber Optics* (Academic Press, 5th Ed., 2012).

[10] J. M. Dudley, G. Genty, and S. Coen, Rev. Mod. Phys. **78**, 1135 (2006); J. M. Dudley and J. R. Taylor, *Supercontinuum Generation in Optical Fibers* (Cambridge University Press, Cambridge, 2010).

[11] W. Wadsworth, N. Joly, J. Knight, T. Birks, F. Biancalana, P. Russell, Opt. Express, **12**, 299-309 (2004).

[12] B. Barviau, B. Kibler, A. Kudlinski, A. Mussot, G. Millot, A. Picozzi, Opt. Express **17**, 7392 (2009).

[13] J. Garnier, M. Lisak, and A. Picozzi, J. Opt. Soc. Am. B **29**, 2229 (2012).

[14] C. Conti, M. A. Schmidt, P. St. J. Russell, and F. Biancalana, Phys. Rev. Lett. **105**, 263902 (2010).

[15] S.V. Manakov, Sov. Phys. JETP **40**, 269 (1975).